

Ultrafast structural dynamics of pyrrole trimer probed by Coulomb explosion imaging

Lu Wu(武璐), Di Zhou(周迪), Shengpeng Zhou(周胜鹏), Zejin Liu(刘泽槿), Xinhui Wang(王馨慧), Jiaqi Zhou(周家琪), Xiaoge Zhao(赵晓戈), Xiyue Lu(卢喜悦), Xiaokai Li(李孝开), Yizhang Yang(杨译章), Xueguang Ren(任雪光), Lanhai He(赫兰海), and Chuncheng Wang(王春成)

Citation: Chin. Phys. B, 2026, 35 (**4**): 043302. DOI: 10.1088/1674-1056/ae3556
http://cpb.iphy.ac.cn; http://iopscience.iop.org/cpb

What follows is a list of articles you may be interested in

Time-dependent quantum wave packet simulation for strong laser-induced molecular dynamics in multiple electronic states of H_2 molecules

Jin-Peng Ma(马金鹏), Xiao-Qing Hu(胡晓青), Yong Wu(吴勇), and Jian-Guo Wang(王建国)
Chin. Phys. B, 2025, 34 (**10**): 103301. DOI: 10.1088/1674-1056/adf319

Time-energy distribution of photoelectron from atomic states with different magnetic quantum numbers in elliptically polarized laser fields

Jingyang Xu(徐菁阳), Li Guo(郭丽), Xin Qi(齐昕), Ronghua Lu(陆荣华), Min Zhang(张敏), Jingtao Zhang(张敬涛), and Jing Chen(陈京)
Chin. Phys. B, 2024, 33 (**9**): 093301. DOI: 10.1088/1674-1056/ad58b3

Comparative study of photoionization of atomic hydrogen by solving the one- and three-dimensional time-dependent Schrödinger equations

Shun Wang(王顺), Shahab Ullah Khan, Xiao-Qing Tian(田晓庆), Hui-Bin Sun(孙慧斌), and Wei-Chao Jiang(姜维超)
Chin. Phys. B, 2021, 30 (**8**): 083301. DOI: 10.1088/1674-1056/abea85

Effect of laser polarization on strong-field ionization and fragmentation of nitrous oxide molecules

Rui Wang(王瑞), Shi-Wen Zhang(张世文), Yang Liu(刘洋), Tian Sun(孙添), Hang Lv(吕航), Hai-Feng Xu(徐海峰)
Chin. Phys. B, 2019, 28 (**5**): 053301. DOI: 10.1088/1674-1056/28/5/053301

Enhanced ionization of vibrational hot carbon disulfide molecules in strong femtosecond laser fields

Wan-Long Zuo(左万龙), Hang Lv(吕航), Hong-Jing Liang(梁红静), Shi-Min Shan(单石敏), Ri Ma(马日), Bing Yan(闫冰), Hai-Feng Xu(徐海峰)
Chin. Phys. B, 2018, 27 (**6**): 063301. DOI: 10.1088/1674-1056/27/6/063301

SPECIAL TOPIC — Ultrafast physics in atomic, molecular and optical systems

Ultrafast structural dynamics of pyrrole trimer probed by Coulomb explosion imaging

Lu Wu(武璐)[1,†], Di Zhou(周迪)[1,†], Shengpeng Zhou(周胜鹏)[1], Zejin Liu(刘泽槿)[1], Xinhui Wang(王馨慧)[1], Jiaqi Zhou(周家琪)[2], Xiaoge Zhao(赵晓戈)[1], Xiyue Lu(卢喜悦)[1], Xiaokai Li(李孝开)[1], Yizhang Yang(杨译章)[1], Xueguang Ren(任雪光)[2], Lanhai He(赫兰海)[1,‡], and Chuncheng Wang(王春成)[1,§]

[1] *Institute of Atomic and Molecular Physics, and Jilin Provincial Key Laboratory of Applied Atomic and Molecular Spectroscopy, Jilin University, Changchun* 130012, *China*

[2] *MOE Key Laboratory for Nonequilibrium Synthesis and Modulation of Condensed Matter, School of Physics, Xi'an Jiaotong University, Xi'an* 710049, *China*

(Received 14 November 2025; revised manuscript received 28 December 2025; accepted manuscript online 8 January 2026)

The ultrafast structural dynamics of the pyrrole trimer induced by femtosecond laser pulses have been investigated using the Coulomb explosion imaging technique. Coincidence measurements of the three-body dissociation channel ($(C_4H_5N)_3^{3+} \rightarrow 3\ C_4H_5N^+$) reveal the geometric configuration and fragmentation behavior of the trimer in the gas phase. Analysis of the kinetic energy release (KER) and fragment angular distributions, combined with Dalitz-plot reconstruction, indicates that the pyrrole trimer predominantly adopts a stable equilateral triangular (cyclic) configuration. *Ab initio* molecular dynamics (AIMD) simulations show that the experimental KER distribution can be reproduced only when the structural evolution proceeds along the ground state of the trimer dication within ~ 50 fs. These results demonstrate that significant intracluster structural rearrangement occurs on an ultrafast timescale during multiple ionization, highlighting the strong coupling between electronic excitation and nuclear motion even in relatively large molecular clusters.

Keywords: strong-field ionization, pyrrole trimer, fragmentation dynamics, Coulomb explosion

PACS: 33.80.Rv, 36.40.–c, 36.40.Wa

DOI: 10.1088/1674-1056/ae3556 **CSTR:** 32038.14.CPB.ae3556

1. Introduction

Molecular clusters, situated between isolated molecules and condensed-phase matter, provide an ideal platform for investigating intermolecular interactions, energy redistribution, and structural stability at the microscopic level.[1–6] As a prototypical hydrogen-bonded aromatic molecule, pyrrole can act as both a hydrogen-bond donor and acceptor, and its molecular skeleton is closely related to biologically important macrocyclic systems such as porphyrins and heme.[7,8] Consequently, elucidating the geometric configurations of pyrrole clusters is crucial for understanding molecular recognition, biomimetic architectures, and strong-field laser–matter interactions.

In recent years, systematic progress has been achieved in the study of pyrrole clusters. Early investigations combining spectroscopy with quantum-chemical calculations revealed the existence and cooperative effects of N–H$\cdots\pi$ interactions in pyrrole dimers, trimers, and larger aggregates. These findings were corroborated by infrared and Raman spectroscopic measurements as well as theoretical analysis.[9,10] Subsequent theoretical studies and molecular dynamics simulations further demonstrated that N–H$\cdots\pi$ hydrogen bonds are preserved during the transition from clusters to the liquid phase.[1] Moreover, experiments employing supersonic jet expansion and matrix isolation techniques showed that stepwise complexation with nitrogen molecules can effectively reproduce the vibrational frequency shifts of pyrrole observed between gas-phase and matrix environments,[11] thereby establishing a continuous model for understanding weak hydrogen bonding and matrix effects.

Coulomb explosion imaging (CEI) is a powerful technique capable of reconstructing the initial geometries of gas-phase molecules and clusters with femtosecond temporal resolution.[12–16] In CEI, intense laser pulses rapidly remove multiple electrons from the target, inducing strong Coulomb repulsion among the resulting ionic fragments and driving subsequent fragmentation.[17–21] By recording the three-dimensional momenta of all fragments in coincidence, the spatial configuration prior to explosion can be inferred. CEI has been successfully applied to small molecules, hydrogen-bonded dimers, and van der Waals clusters, revealing structural information often inaccessible to conventional spectroscopic methods.[12,18,22–30] These studies have demonstrated the unique capability of CEI to capture transient configurations

[†]These authors contributed equally to this work.

[‡]Corresponding author. E-mail: helanhai@jlu.edu.cn

[§]Corresponding author. E-mail: ccwang@jlu.edu.cn

© 2026 Chinese Physical Society and IOP Publishing Ltd. All rights, including for text and data mining, AI training, and similar technologies, are reserved.

and ultrafast structural rearrangements during strong-field interactions.

In this work, we perform high-resolution coincidence measurements of the three-body Coulomb explosion of neutral pyrrole trimers in the gas phase. Conformational candidates obtained from GMMX searches in Gaussian[31] were used to identify the three lowest-energy isomers, which were subsequently employed for classical Coulomb-explosion and Dalitz-plot simulations. Comparison with the measured kinetic energy release (KER) and fragment momentum distributions, together with Dalitz-plot analysis, reveals that the pyrrole trimer is dominated by a cyclic equilateral-triangle configuration. *Ab initio* molecular dynamics (AIMD)[32–35] simulations based on the same initial geometries reproduce the experimental KER distribution only when ultrafast structural evolution along the ground-state dication potential occurs within ~ 50 fs. The combined experimental and theoretical results consistently demonstrate that the pyrrole trimer adopts a stable cyclic triangular structure in the gas phase, enabling reconstruction of its initial geometry prior to ionization. These findings not only clarify the structural motif of the pyrrole trimer but also raise intriguing questions about how strong-field ionization drives structural rearrangement in hydrogen-bonded molecular clusters — a topic that warrants further exploration.

2. Experimental methods

The ultrafast structural dynamics of the pyrrole trimer induced by femtosecond laser pulses were investigated using a cold target recoil ion momentum spectroscopy (COLTRIMS) apparatus. In the experiment, helium gas at a backing pressure of 2 bar was bubbled through liquid pyrrole at room temperature and subsequently expanded into a vacuum chamber through a 30 μm nozzle, generating a molecular beam containing pyrrole trimer in the interaction region.[36–38] The translational temperature of the sample beam was estimated to be approximately 42 K from the longitudinal momentum spread of the produced ions along the jet propagation axis. A linearly polarized femtosecond laser pulse with a central wavelength of 800 nm and a pulse duration of 55 fs was focused onto the target using a concave mirror with a focal length of 75 mm, yielding a focused spot size of approximately 8 μm and a peak intensity of 300 TW/cm^2. The laser field ionized and dissociated the pyrrole trimers within the COLTRIMS spectrometer, enabling momentum-resolved detection of all ionic fragments. The fragments were further selected according to momentum conservation to isolate the coincidence channel

$$(C_4H_5N)_3^{3+} \rightarrow C_4H_5N^+ + C_4H_5N^+ + C_4H_5N^+.$$

3. Theoretical model

AIMD simulations were performed using the Gaussian09 software package. Conformational searches were first carried out with the GMMX module using the MMFF94 force field, with an energy threshold of 3.5 kcal/mol and a maximum of 10000 search steps. To further refine the structural and energetic details, all candidate geometries identified by GMMX were subsequently optimized at the M06-2X/aug-cc-pVDZ level (optimized structure shown in Fig. 1). Dynamical simulations were conducted for the lowest-energy cyclic equilateral-triangle isomer. Conformational sampling was generated under a Boltzmann distribution at 50 K, and the sampled geometries were used as initial conditions for the dynamics.

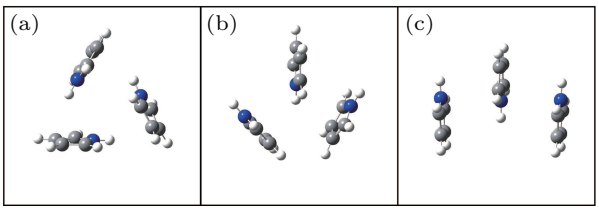


Fig. 1. Schematic representations of the optimized geometries of the pyrrole trimer.

Trajectory propagation was performed using the atom-centered density matrix propagation (ADMP) method at the ωB97XD/6-31G level.[32,39–42] In the simulation, no interatomic distances within the molecules were constrained, in order to accurately capture the dissociation dynamics and to avoid the artifact whereby all Coulomb potential energy is converted into translational kinetic energy of the center-of-mass motion. Evolution on the dicationic potential-energy surface resulted in ionization and subsequent dissociation within approximately 50 fs.

To evaluate the total KER, the kinetic energies of the resulting ionic fragments were summed and augmented by the residual Coulomb potential energy calculated from the distances between their centers of mass.

4. Results and discussion

Upon rapid removal of three electrons from the equilibrium geometry, the initially bound pyrrole trimer transitions into a Coulomb-repulsive state and undergoes prompt dissociation. The resulting ionic fragments were selected according to momentum conservation, enabling clear identification of the dissociation channel $C_4H_5N^+ + C_4H_5N^+ + C_4H_5N^+$, as illustrated in Fig. 2. In this plot, the horizontal axis represents the time-of-flight (TOF) of the first ion, while the vertical axis corresponds to the sum of the TOFs of the second and third ions. The broadened lines in the spectrum are attributed to the emission of neutral pyrrole fragments during dissociation, whereas vertical and horizontal streaks arise from accidental

coincidences. The dashed lines and their associated distributions are assigned to channels involving the ^{13}C isotope.

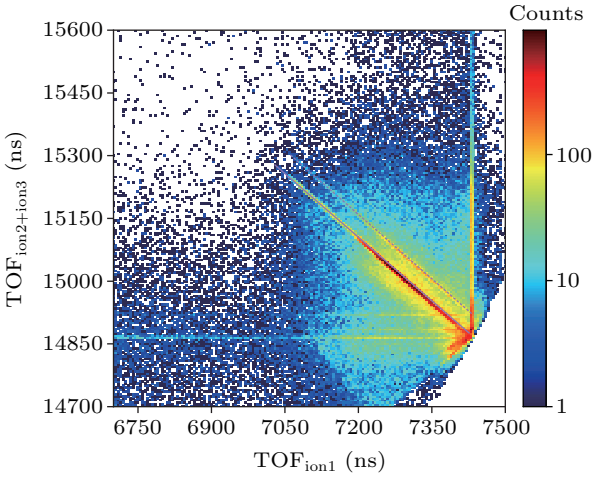


Fig. 2. Time-of-flight coincidence map for the dissociation of $(C_4H_5N)_3^{3+}$. Solid lines indicate the dissociation channel $(C_4H_5N)_3^{3+} \rightarrow C_4H_5N^+ + C_4H_5N^+ + C_4H_5N^+$, while the dashed lines correspond to the ^{13}C isotopic channel.

The three-body dissociation channel can generally proceed via either a sequential or a concerted fragmentation mechanism. In the sequential pathway, the parent ion first dissociates into an intermediate species before further fragmentation, which violates the recoil approximation. Consequently, the measured fragment momenta no longer accurately reflect the initial geometry of the neutral trimer. To clarify the dissociation dynamics of the pyrrole trimer under Coulomb explosion, we first examined the momentum correlations among the three ionic fragments.

To determine the initial geometry of the pyrrole trimer, standard momentum-correlation analysis tools — the Dalitz plot and the Newton diagram — were employed (Fig. 3). In the Dalitz representation (Fig. 3(a)), the kinetic energies of the three fragments are projected into an equilateral-triangle coordinate system, with coordinates defined as

$$X = \frac{E_1 - E_2}{\sqrt{3}E_k}, \quad Y = \frac{E_3}{E_k} - \frac{1}{3},$$

where E_1, E_2, and E_3 denote the kinetic energies of the individual fragments and E_k is the total kinetic energy. This representation clearly reveals energy correlations among the three fragments. The experimental data show that the pyrrole trimer predominantly lies around the origin $(0,0)$, indicating near-equal partitioning of kinetic energy and simultaneous fragment release, consistent with a concerted three-body dissociation. From this observation, one may reasonably infer that the inter-centroid distances among the three pyrrole monomers in the precursor trimer are effectively equal.

In the Newton-diagram analysis, the momentum direction of the first detected fragment was defined as the positive x-axis and normalized to unity, with the momenta of the remaining two fragments scaled and compared in the same frame. The normalized distribution exhibits equal momentum magnitudes for all three fragments, with mutual angles of approximately 120° between them. This momentum geometry directly corresponds to an equilateral-triangle configuration, providing further support for a concerted dissociation originating from a cyclic equilateral-triangle initial structure.

To exclude contributions from alternative isomers, Dalitz plots were simulated for the three candidate geometries shown in Fig. 1 under the assumption of concerted dissociation (Fig. 4). Because identical-mass fragments cannot be uniquely labeled experimentally, fragment indices were randomly permuted in the simulation to reflect indistinguishability. Comparison between the simulated and experimental Dalitz distributions shows that only the cyclic equilateral-triangle isomer produces clustering at the origin, in agreement with the momentum-correlation analysis. These results demonstrate that the pyrrole trimer in the molecular beam predominantly adopts a cyclic equilateral-triangle configuration.

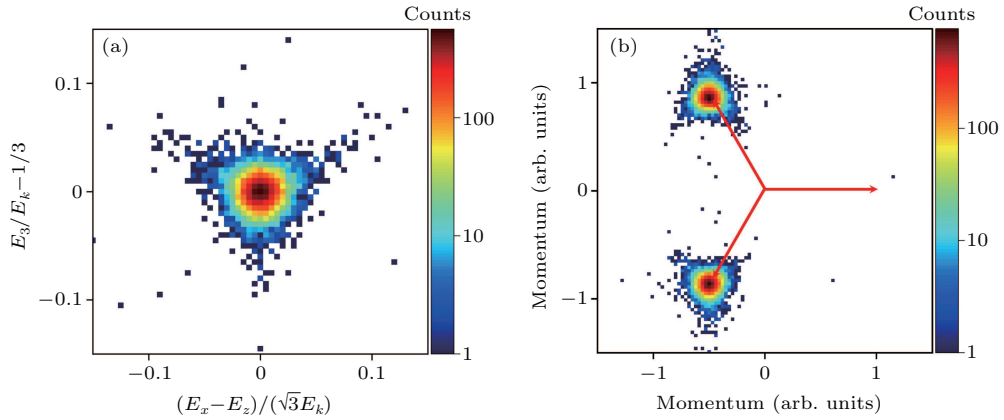


Fig. 3. Energy and momentum correlation maps for the three-body dissociation of the pyrrole trimer. (a) Dalitz plot with $X = (E_x - E_z)/(\sqrt{3}E_k)$ and $Y = E_y/E_k - 1/3$; the high-density region at the center indicates near-equal kinetic-energy partitioning and synchronous fragment release. (b) Newton diagram showing momentum vectors of the three ions; red arrows indicate momentum, with mutual angles of $\sim 120°$, consistent with an equilateral-triangle geometry.

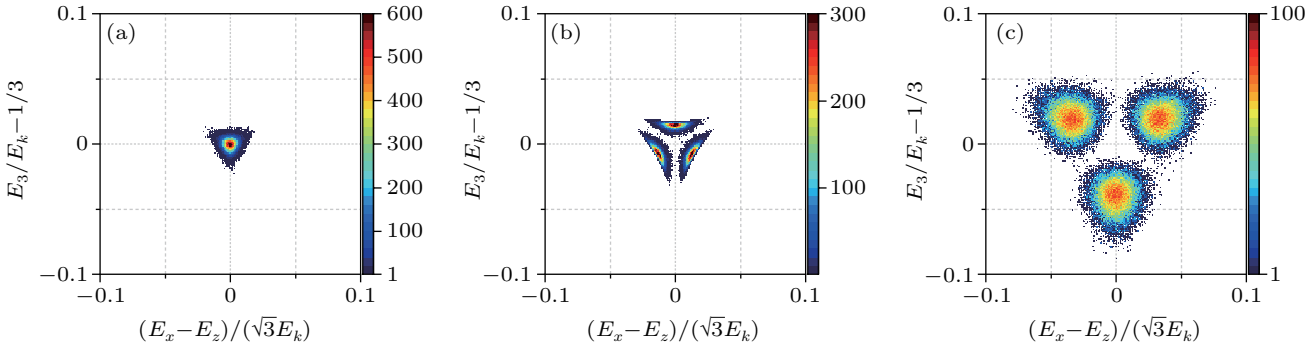


Fig. 4. Simulated Dalitz plots for the pyrrole trimer based on different initial structures, assuming concerted three-body dissociation.

To further validate this assignment, AIMD simulations were performed. The neutral trimer geometry was first optimized using standard cluster-conformation search methods, yielding the lowest-energy equilateral-triangle structure. Starting from this optimized geometry, three electrons were removed to construct the tricationic system, and trajectories were propagated at 50 K with a time step of $\Delta t = 0.5$ fs for a total duration of 500 fs. The initial sampling and the electron-removal protocol were chosen to ensure consistency with the experimental conditions.

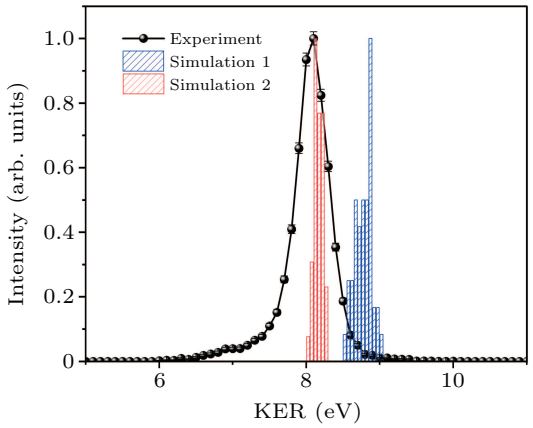


Fig. 5. KER distributions for the pyrrole trimer. The black dotted line denotes the experimental data. The blue histogram corresponds to vertical ionization of the neutral geometry to the tricationic state, while the red histogram represents vertical ionization to the dicationic ground state followed by ∼ 50 fs evolution and subsequent ionization to the tricationic state. The error bars indicate the statistical uncertainty.

The simulated total KER distribution was then compared with the experimental data (Fig. 5). Direct vertical ionization simulation to the tricationic state yields a KER peak at 8.8 eV, whereas the experimental peak is at 8.1 eV, a discrepancy of approximately 0.7 eV. This difference is primarily attributed to the vertical-ionization approximation, which neglects laser-envelope-induced bond elongation and ultrafast structural evolution during ionization. When the neutral geometry is instead vertically ionized to the dicationic ground state and allowed to evolve on that surface for ∼ 50 fs prior to further ionization and dissociation, the resulting KER distribution shows good agreement with experimental data. During this ultrafast evolution, the center-of-mass distance between pyrrole units stretched by approximately 0.12 Å. This observation indicates that ultrafast structural evolution plays a significant role in determining the final energy partitioning in multiple-ionization processes.

5. Conclusions

The fragmentation dynamics of pyrrole trimers in the gas phase have been elucidated by Coulomb explosion imaging, with experimental identification of a symmetric three-body dissociation channel and momentum-resolved measurements enabling precise reconstruction of the initial molecular geometry. Complementary AIMD further confirmed the cyclic equilateral-triangle configuration and accurately reproduced the observed kinetic energy distributions. These findings demonstrate that the pyrrole trimer adopts a stable cyclic triangular arrangement in the gas phase and establish a reliable framework for investigating ultrafast structural evolution in weakly bound systems. Moreover, the combined experimental and theoretical approach highlights the critical role of electron-nuclear coupling in driving ultrafast structure rearrangements during multiple ionization, suggesting that similar mechanisms may govern the dynamics of larger hydrogen-bonded molecular clusters under strong-field conditions.

Acknowledgments

Project supported by the Innovation Program for Quantum Science and Technology (Grant No. 2024ZD0300700) and the National Natural Science Foundation of China (Grant Nos. 12525411, 92261201, 12274179, 12325406, and 12334011).

References

[1] Gao W, Feng H, Xuan X and Chen L 2012 *Mol. Phys.* **110** 2151
[2] Johny M, Schouder C A, Al-Refaie A, He L, Wiese J, Stapelfeldt H, Trippel S and Küpper J 2024 *Phys. Chem. Chem. Phys.* **26** 13118
[3] Zhou J, Jia S, Xue X, *et al.* 2024 *J. Phys. Chem. Lett.* **15** 1529
[4] Yang T, Zhang X, Li X, Li W, Wei M, Zhang D, He L and Ding D 2025 *Chin. Phys. B* **34** 033302
[5] Qu Q, Sun F, Wang J, Gao J, Li H and Wu J 2024 *Chin. Phys. B* **33** 047803

[6] Wang C, Waters M D, Zhang P, Suchan J, Svoboda V, Luu T T, Perry C, Yin Z, Slavíček P and Wörner H J 2022 *Nat. Chem.* **14** 1126
[7] Poulos T L 2014 *Chem. Rev.* **114** 3919
[8] Paolesse R, Nardis S, Monti D, Stefanelli M and Di Natale C 2017 *Chem. Rev.* **117** 2517
[9] Dauster I, Rice C A, Zielke P and Suhm M A 2008 *Phys. Chem. Chem. Phys.* **10** 2827
[10] Matsumoto Y and Honma K 2009 *J. Chem. Phys.* **130**
[11] Oswald S, Suhm M A and Coussan S 2019 *Phys. Chem. Chem. Phys.* **21** 1277
[12] Yu X, Liu Y, Deng K, Zhang X, Ma P, Li X, Wang C, Cui Z, Luo S and Ding D 2022 *Phys. Rev. A* **105** 063105
[13] Wu J, Kunitski M, Schmidt L P H, Jahnke T and Dörner R 2012 *J. Chem. Phys.* **137**
[14] Ablikim U, Bomme C, Xiong H, *et al.* 2016 *Sci. Rep.* **6** 38202
[15] Yadav J, Safvan C, Bhatt P, Kumari P, Kumar A and Rajput J 2022 *J. Chem. Phys.* **156**
[16] Xiao F, Wang L, Bai G, Zheng Z, Sun X, Ji T, Sun Y, Wang J, Wang X and Zhao Z 2025 *Chin. Phys. Lett.* **42** 043701
[17] Vager Z, Naaman R and Kanter E 1989 *Science* **244** 426
[18] Lam H V S, Venkatachalam A S, Bhattacharyya S, *et al.* 2024 *Phys. Rev. Lett.* **132** 123201
[19] Ashrafi-Belgabad A, Karimi R, Monfared M, *et al.* 2024 *Commun. Phys.* **7** 405
[20] Wang Z, Hu X, Xue X, *et al.* 2023 *Nat. Commun.* **14** 5420
[21] Liu Z, Zhang M, Zhou T, Li X, Zhou S, Wu L, Yang Y, Zhou J, He L, Zhang D, Ren X, Kuleff A I, Vendrell O, Ueda K, Li Z, Ding D and Wang C 2025 *Nat. Commun. 17* 874
[22] Zeller S, Kunitski M, Voigtsberger J, Waitz M, Trinter F, Eckart S, Kalinin A, Czasch A, Schmidt L P H and Weber T, 2018 *Phys. Rev. Lett.* **121** 083002
[23] Pickering J D, Shepperson B, Hübschmann B A, Thorning F and Stapelfeldt H 2018 *Phys. Rev. Lett.* **120** 113202
[24] Khan A, Jahnke T, Zeller S, Trinter F, Schöffler M, Schmidt L P H, Dörner R and Kunitski M 2020 *J. Phys. Chem. Lett.* **11** 2457
[25] Légaré F, Lee K F, Litvinyuk I, Dooley P, Wesolowski S, Bunker P, Dombi P, Krausz F, Bandrauk A and Villeneuve D M 2005 *Phys. Rev. A* **71** 013415
[26] Luzon I, Livshits E, Gope K, Baer R and Strasser D 2019 *J. Phys. Chem. Lett.* **10** 1361
[27] Wang J, Mi X, Liang Z, Dong B, Deng Y, Zhang M, Li Z and Liu Y 2025 *J. Am. Chem. Soc.* **147** 20302
[28] Zhao X, Zhang X, Liu H, Ma P, Li X, Wang C, Luo S and Ding D 2025 *Phys. Rev. A* **111** 053106
[29] Li X, Yu X, Ma P, Zhao X, Wang C, Luo S and Ding D 2022 *Chin. Phys. B* **31** 103304
[30] Christiansen L, Nielsen J H, Christensen L, Shepperson B, Pentlehner D and Stapelfeldt H 2016 *Phys. Rev. A* **93** 023411
[31] Frisch M, Trucks G W and Schlegel H B, *et al.* 2009 *Gaussian 09, Revision D.01* (Gaussian Inc.)
[32] Schlegel H B, Millam J M, Iyengar S S, Voth G A, Daniels A D, Scuseria G E and Frisch M J 2001 *J. Chem. Phys.* **114** 9758
[33] Vuilleumier R 2006 *Computer Simulations in Condensed Matter Systems: From Materials to Chemical Biology, Vol. 1* (Springer) pp. 223
[34] Payne M C, Teter M P, Allan D C, Arias T and Joannopoulos J D 1992 *Rev. Mod. Phys.* **64** 1045
[35] Tuckerman M E and Martyna G J 2002 *J. Phys. Chem. B* **104** 159
[36] Jin W, Wang C, Zhao X, Yang Y, Ren D, Liu Z, Li X, Luo S and Ding D 2024 *Chin. Phys. Lett.* **41** 053101
[37] Zhou J, Wu L, Belina M, Skitnevskaya A D, Jia S, Xue X, Hao X, Zeng Q, Ma Q and Zhao Y 2025 *Nat. Commun.* **16** 5838
[38] Yang Y, Ren H, Zhang M, Zhou S, Mu X, Li X, Wang Z, Deng K, Li M and Ma P 2023 *Nat. Commun.* **14** 4951
[39] Wang Y, Wang E, Zhou J, Dorn A and Ren X 2021 *J. Chem. Phys.* **154**
[40] Schlegel H B, Iyengar S S, Li X, Millam J M, Voth G A, Scuseria G E and Frisch M J 2002 *J. Chem. Phys.* **117** 8694
[41] Iyengar S S, Schlegel H B, Millam J M, Voth G A, Scuseria G E and Frisch M J 2001 *J. Chem. Phys.* **115** 10291
[42] Iyengar S S, Schlegel H B, Voth G A, Millam J M, Scuseria G E and Frisch M J 2002 *Isr. J. Chem.* **42** 191